A Kinetic and Thermodynamic Study of the Glycosidic Bond Cleavage in Deoxyuridine

Andrea L. Millen,[†] Laura A. B. Archibald,[†] Ken C. Hunter,[†] and Stacey D. Wetmore*[,‡]

Department of Chemistry, Mount Allison University, 63C York Street, Sackville, New Brunswick E4L 1G8, Canada, and Department of Chemistry and Biochemistry, University of Lethbridge, 4401 University Drive, Lethbridge, Alberta T1K 3M4, Canada

Received: June 20, 2006; In Final Form: December 21, 2006

Density functional theory was used to study the thermodynamics and kinetics for the glycosidic bond cleavage in deoxyuridine. Two reaction pathways were characterized for the unimolecular decomposition in vacuo. However, these processes are associated with large reaction barriers and highly endothermic reaction energies, which is in agreement with experiments that suggest a (water) nucleophile is required for the nonenzymatic glycosidic bond cleavage. Two (S_N1 and S_N2) reaction pathways were characterized for direct hydrolysis of the glycosidic bond by a single water molecule; however, both pathways also involve very large barriers. Activation of the water nucleophile via partial proton abstraction steadily decreases the barrier and leads to a more exothermic reaction energy as the proton affinity of the molecule interacting with water increases. Indeed, our data suggests that the barrier heights and reaction energies range from that for hydrolysis by water to that for hydrolysis by the hydroxyl anion, which represents the extreme of (full) water activation (deprotonation). Hydrogen bonds between small molecules (hydrogen fluoride, water, or ammonia) and the nucleobase were found to further decrease the barrier and overall reaction energy but not to the extent that the same hydrogen-bonding interactions increase the acidity of the nucleobase. Our results suggest that the nature of the nucleophile plays a more important role in reducing the barrier to glycosidic bond cleavage than the nature of the small molecule bound, and models with more than one hydrogen fluoride molecule interacting with the nucleobase provide further support for this conclusion. Our results lead to a greater fundamental understanding of the effects of the nucleophile, activation of the nucleophile, and interactions with the nucleobase for this important biological reaction.

Introduction

The cleavage of glycosidic bonds in DNA is an important process that occurs with great frequency in nature. However, the stability of DNA causes this to be a high-energy reaction, which requires catalysis by various enzymes.[1−3] For example, the DNA glycosylases, which are involved in DNA repair pathways, cleave glycosidic bonds to remove damaged nucleobases from the double helix. Alternatively, nucleoside hydrolases and phosphorylases, which are involved in nucleoside salvage pathways, break glycosidic bonds to recycle bases for future use.[3]

The proposed mechanisms for enzymes that catalyze DNA (and RNA) glycosidic bond cleavages bear many similarities. In particular, due to the stability of nucleotides, proposed mechanisms involve attack of a nucleophile (for example, water in the case of hydrolases,[5,9−11,15−17,19,24−27] ricin toxin A-chain,[7,28] and some DNA glycosylases (UDG[8,29−32] or MutY[33]), an active site (amine) amino acid in some DNA glycosylases (hOGG1[22,34,35] or FPG[36,37]), and hydrogen phosphate in phosphorylases[6,12−14,18,20,21,23,38−40]). It is sometimes proposed that this nucleophile is activated via proton abstraction by an amino acid residue.[1,2,9−11,17,26] Some mechanisms for enzyme-catalyzed glycosidic bond cleavage involve the proposed formation of oxocarbenium-like transition states.[1,2] For example, the proposed mechanism of action of the best studied DNA glycosylase (uracil DNA glycosylase, UDG) involves the formation of a nucleobase anion upon cleavage of the base−sugar bond, and it has been hypothesized that the enzyme stabilizes the anionic intermediate through hydrogen-bonding interactions with active site residues.[1,2,29] Furthermore, although some glycosylases (MutY) have been proposed to protonate purines (adenine) prior to base departure,[1,2,33] there is evidence that other (damaged) purines (8-oxoguanine) may be repaired through anionic intermediates.[41] Additionally, most mechanisms involve (at least partial) stabilization of the departing nucleobase through hydrogen-bonding interactions with active site amino acids.[1,2,9−11,14,18,21−23,26,27,29,31−34,37,38]

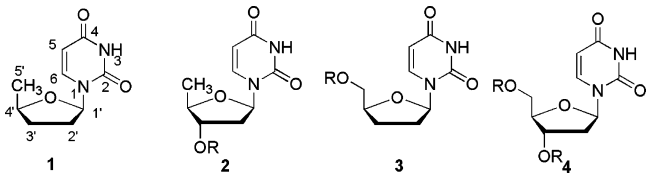

Figure 1. Deoxyribose sugar models investigated in the present work (R = H or CH_3).

In an attempt to better understand the role of nucleobase activation in the glycosidic bond cleavage process, previous work in our lab has considered the effects of hydrogen bonding on the acidity of the natural, as well as damaged, nucleobases.[42,43] The effects of hydrogen-bonding interactions on the acidity (N1 for the pyrimidines or N9 for the purines) were investigated due to the proposed formation of the base anion along the reaction pathway for the best studied glycosylase (UDG) and the relationship between the acidity and the leaving

* Author to whom correspondence should be addressed. E-mail: stacey.wetmore@uleth.ca.
[†] Mount Allison University.
[‡] University of Lethbridge.

10.1021/jp063841m CCC: $37.00
Published on Web 03/17/2007

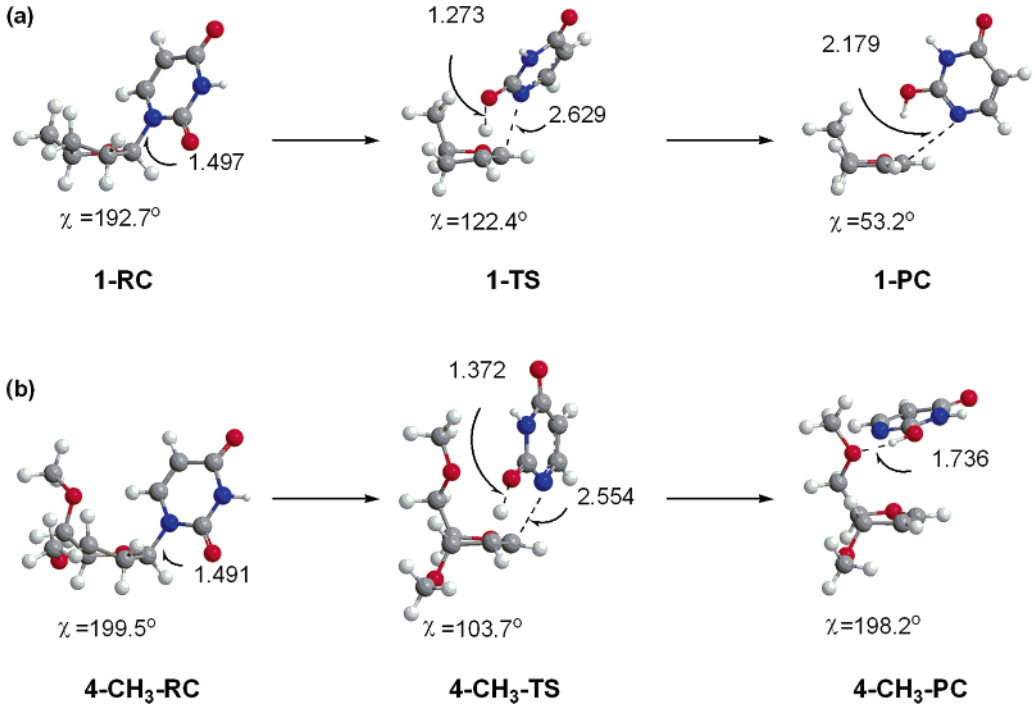

Figure 2. Selected B3LYP/6-31G(d) bond lengths (Å) and dihedral angles ($\chi = \angle$(O4′−C1′−N1−C2), deg) in reactant (RC), transition state (TS), and product (PC) complexes for the unimolecular decomposition of deoxyuridine (in vacuo) that involves abstraction of C2′−H studied using models (a) **1** and (b) **4-CH$_3$**.

TABLE 1: Barriers and Reaction Energies (kJ mol^{-1}) for the Unimolecular Decomposition of Deoxyuridine in Vacuo[a]

	C2′−H abstraction[c]		direct C1′−N1 cleavage[d]	
model[b]	barrier	reaction energy	barrier	reaction energy
1	150.9	80.8	168.7	65.9
4-CH$_3$	156.3	65.2	188.6	74.3

[a] B3LYP/6-311+G(2d,p)//B3LYP/6-31G(d) relative energies include scaled (0.9806) ZPVE corrections. [b] See Figure 1 for model nomenclature. [c] See Figure 2. [d] See Figure 3.

ability of the base. Although this is an important approach, our previous work focused only on the properties of the nucleobases, and therefore extended models must be considered to determine, for example, the effects of hydrogen bonding on the kinetics of the glycosidic bond cleavage process as well as the effects of the nucleophile.

Computational chemistry can provide useful information about short-lived transition states that is difficult to obtain from experiments. Indeed, a number of studies have used computational chemistry to investigate glycosidic bond cleavage pathways.[7,9,12,16−18,20−22,25,32,35] However, these studies have generally focused on only one feature of the glycosidic bond cleavage catalyzed by a specific enzyme. Due to the similarities in the proposed mechanisms for many of these enzymes, our desire is to study the fundamentals of this reaction independent of the interactions within a particular active site.

In the present study, we consider the general mechanism of glycosidic bond cleavage in deoxyuridine. Deoxyuridine was chosen due to the small size of the nucleobase and the lack of a systematic study in the literature investigating appropriate computational models for the glycosidic bond cleavage process. We will consider the direct unimolecular decomposition as well as the glycosidic bond cleavage involving a water nucleophile. Water was chosen as the nucleophile due to the importance of water in nature and its anticipated role in the glycosidic bond cleavage catalyzed by several enzymes.[5,7−11,15−17,19,24−33] Finally, the effects of hydrogen-bonding interactions with the nucleophile and/or nucleobase on the reaction path will be considered. Our systematic approach will complement our previous work by revealing the effects of hydrogen-bonding interactions on both the thermodynamics and the kinetics of this important biological reaction.

Computational Details

In our previous work,[42,43] gas-phase geometries were obtained using the B3LYP[44] method in conjunction with the 6-31+G(d,p) basis set. Although diffuse functions have been shown to be required to properly describe anionic hydrogen-bonded systems, the use of diffuse functions on larger models becomes increasingly computationally expensive. As our goal is to extend our models in future work to adequately depict active site interactions, it would be beneficial to identify a reduced basis set with equal accuracy. Therefore, Figures S1−S3 in the Supporting Information compare the B3LYP geometries of the reactant, transition state, and product complexes optimized with the 6-31G(d) and 6-31+G(d,p) basis sets, while Tables S1−S4 compare the B3LYP/6-311+G(2d,p) barriers and reaction energies calculated using both basis sets. The results clearly indicate that for a variety of different reaction pathways and model systems, the geometries and corresponding energetics are not highly dependent upon the basis set used in the geometry optimization. Therefore, our discussion focuses on the 6-31G(d) geometries.

In addition to the level of theory, we must identify an appropriate deoxyribose sugar model to study the glycosidic bond cleavage within nucleotides. Small, noncyclic models have been previously used to investigate the depurination of deoxyadenosine by ricin toxin A-chain.[7] Although we initially considered similar small models in hopes to reduce the complexity of our calculations, we did not find this approach to be viable due to unfavorable interactions between the base and the model sugar that do not exist when deoxyuridine is incorporated into a DNA helix. Therefore, we focus our attention on four substituted tetrahydrofuran models (Figure 1). In our

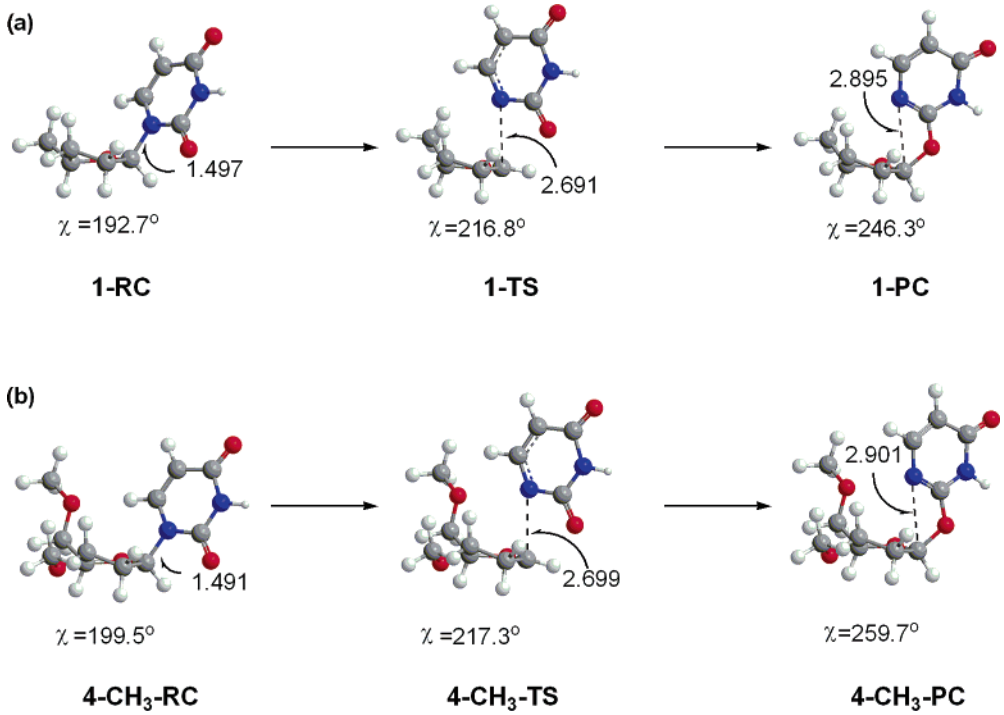

Figure 3. Selected B3LYP/6-31G(d) bond lengths (Å) and dihedral angles ($\chi = \angle$(O4′−C1′−N1−C2), deg) in reactant (RC), transition state (TS), and product (PC) complexes for the unimolecular decomposition of deoxyuridine (in vacuo) that involves direct cleavage of the C1′−N1 glycosidic bond studied using models (a) **1** and (b) **4-CH$_3$**.

models, the DNA phosophodiester groups at C3′ and C5′ are replaced with hydrogen and/or hydroxyl groups.[45] This approach eliminates difficulties associated with modeling charged and conformationally flexible phosphate groups and thereby allows us to focus on the effects of the deoxyribose sugar.

Using all four models, we studied the unimolecular glycosidic bond cleavage in deoxyuridine in vacuo and the hydrolysis of the glycosidic bond by the hydroxyl anion. Comparison of the geometries of reactant, transition state and product complexes for the different models indicates that hydroxyl groups at C5′ and C3′ are inefficient models for DNA phosophodiesters due to interactions with the nucleobase (Figures S1−S3) or nucleophile (Figure S3) that are not possible within DNA. Although stable transition states or product complexes could not be isolated with the hydroxyl groups directed away from the nucleobase and/or nucleophile, methoxyl groups were found to stabilize more relevant structures (models denoted as **2-CH$_3$**, **3-CH$_3$** and **4-CH$_3$**, Figures S2 and S3 in the Supporting Information). Indeed, the C4′−C5′−O5′−C_{CH_3} and C4′−C3′−O3′−C_{CH_3} dihedral angles remain near 182° (±6°) throughout the reaction with the exception of the C4′−C3′−O3′−C_{CH_3} dihedral angle in one product complex, which equals 162°. Since the geometries (Figures S1−S3) and relative energies (Tables S1−S3) for models **1** and **4-CH$_3$** are similar, we conclude that model **1** will be useful in future studies when limited by computational resources, while methoxyl groups at C5′ and C3′ (model **4-CH$_3$**) can be used if sufficient resources are available and the effects of the C3′ and C5′ substituents in DNA must be considered.

On the basis of the above results, we perform higher-level B3LYP/6-311+G(2d,p) single-point calculations on B3LYP/6-31G(d)-optimized geometries. We use both our smallest (model **1**) and largest (**4-CH$_3$**) models for comparison of different reaction pathways. Frequency calculations were performed at the same level of theory as the optimizations, and scaled (0.9806) zero-point vibrational energy (ZPVE) corrections were added to all relative energies. Each single-point calculation on hydrogen-bonded complexes includes a correction for basis set superposition error (BSSE) as described by the Boys and Bernardi counterpoise method.[46] Transition structures containing only one imaginary vibrational frequency were isolated. To confirm that this frequency corresponds to the desired reaction coordinate, the reaction paths from the transition states were followed using intrinsic reaction coordinate (IRC) calculations. The end points from the IRC calculations were then optimized to ensure a minimum with all real vibrational modes was obtained for both the reactant and product complexes. All calculations were performed with Gaussian 03.[47]

Results and Discussion

Unimolecular Glycosidic Bond Cleavage In Vacuo. It has been well-established that the nucleotides are highly stable molecules and therefore require hydrolysis or enzymatic catalysis to degrade via glycosidic bond cleavage.[1,2] Nevertheless, to gain a greater understanding of the glycosidic bond cleavage process, it is of interest to consider the unimolecular decomposition of deoxyuridine (in vacuo) in the absence of other external forces.

In vacuo, the reactant complex for glycosidic bond cleavage (Figure 2) has C3′-endo sugar puckering,[48,49] and the base is in the anti conformation, which is the naturally occurring conformation in DNA.[50] In the transition state, the O2 of uracil partially abstracts a C2′ hydrogen, which is required in the gas phase to stabilize a partial negative charge on the base and a partial positive charge on the sugar. In the product complex, the C2′ hydrogen is completely abstracted by uracil, and a double bond is formed between C1′ and C2′, which flattens the sugar ring. The nucleobase adopts a syn-like orientation and remains coordinated to the sugar moiety through a weak interaction with the newly formed C1′−C2′ double bond in model **1** and a stronger (O5′···H−O2) hydrogen bond in model **4-CH$_3$**.

Although a transition state involving C2′−H abstraction has been previously reported in the computational literature, where

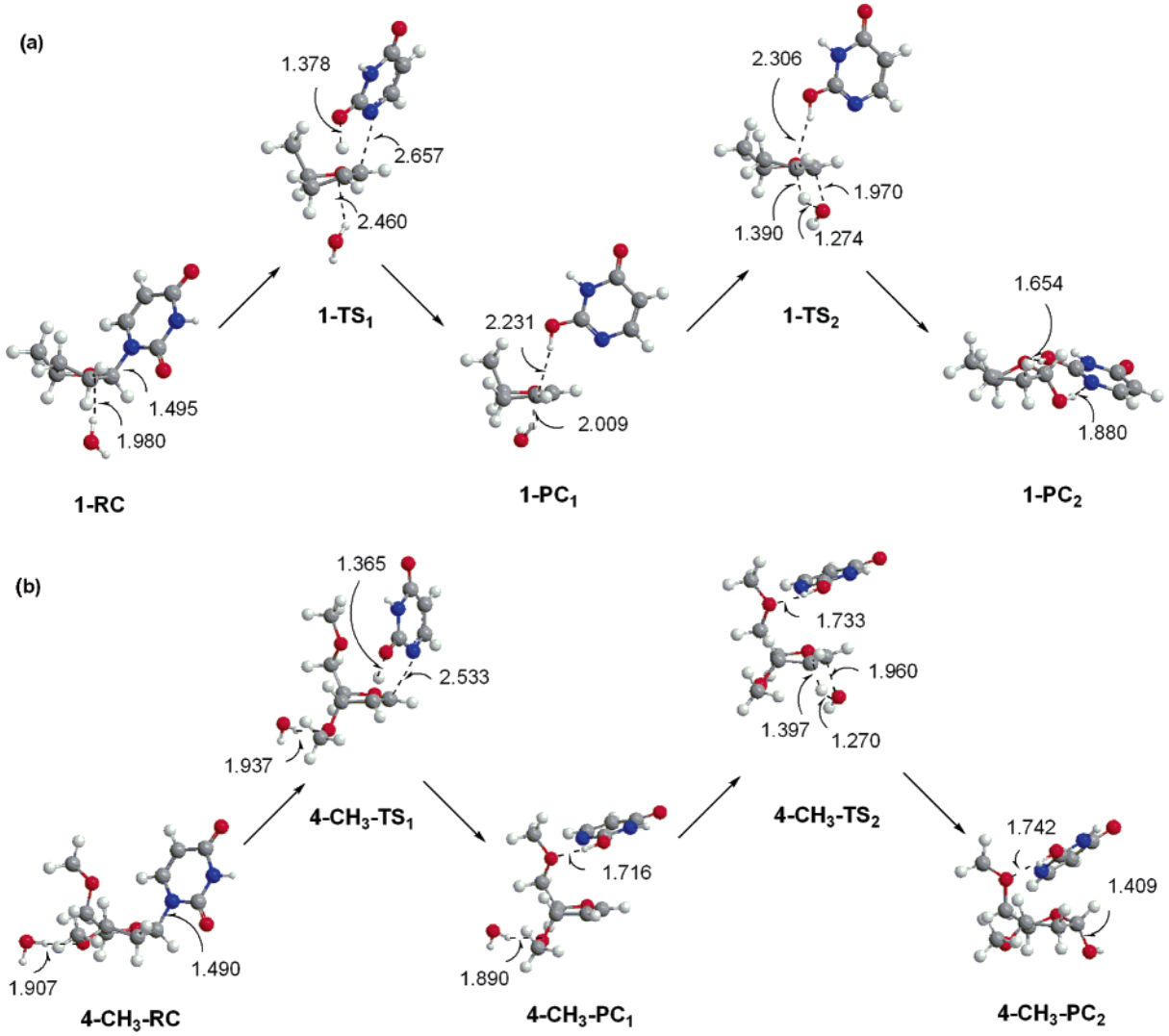

Figure 4. Selected B3LYP/6-31G(d) bond lengths (Å) in reactant (RC), transition state (TS), and product (PC) complexes for the S_N1 pathway for direct hydrolysis of the glycosidic bond in deoxyuridine studied using models (a) **1** and (b) **4-CH$_3$**.

oxoimidazole was used as the nucleobase to model the reaction catalyzed by hOGG1 (a DNA repair enzyme),[22] there is little experimental evidence that glycosidic bond cleavages within nucleotides proceed via high-energy glycal intermediates. Indeed, only one report of a ribal moiety as a minor product in an enzymatic reaction can be found in the literature.[51] Furthermore, this is a high-energy process, where the reaction barrier is approximately 150−155 kJ mol^{-1} (Table 1), and the overall reaction is largely endothermic (65−80 kJ mol^{-1}).

Further searches of the potential energy surface for cleavage of the C1′−N1 glycosidic bond reveals a second possible transition state in vacuo (Figure 3). Despite the promise of this transition structure, this is a higher-energy process than abstraction of the C2′ sugar hydrogen (Table 1). Furthermore, the instability of the (charge) separated sugar cation and base anion in the gas phase leads to bond formation between the O2 carbonyl of the base and C1′ of the sugar moiety in the product complex.

In summary, it is clear from our in vacuo calculations of the unimolecular decomposition of deoxyuridine that direct cleavage of the glycosidic bond is not feasible. This is in agreement with experimental suggestions that the nonenzymatic bond cleavage occurs via hydrolysis and stresses the important role of the nucleophile. We therefore turn our attention to the hydrolysis of the glycosidic bond in deoxyuridine in the following section.

Direct Hydrolysis of the Glycosidic Bond. As discussed in the Introduction, although a range of nucleophiles (water, amines, and phosphates) have been implicated in the glycosidic bond cleavage of nucleotides, water is present in the active sites of many enzymes that catalyze glycosidic bond cleavage reactions.[5,7−11,15−17,19,24−33] Therefore, we investigated the role of water in the decomposition of deoxyuridine and have characterized two mechanisms (in vacuo) by which water is involved in the glycosidic bond cleavage through attack at C1′.

The first pathway is a two-step (S_N1) reaction (Figure 4). In the first step, the C2′−H bond is abstracted by the nucleobase as the glycosidic bond is cleaved, and water is coordinated to O4′ (model **1**) or the C3′ oxygen (model **4-CH$_3$**).[52] In the second step, water adds across the C1′−C2′ double bond, which restores the C2′ hydrogen. We note, however, that there is no experimental evidence for abstraction of a (C2′) sugar hydrogen during the hydrolysis of deoxynucleosides, which suggests that another pathway dominates. The second pathway characterized in the present work is a one-step (S_N2) reaction (Figure 5). For both models, the water molecule simultaneously coordinates to C1′−H and the uracil O2 carbonyl in the reactant complex. As

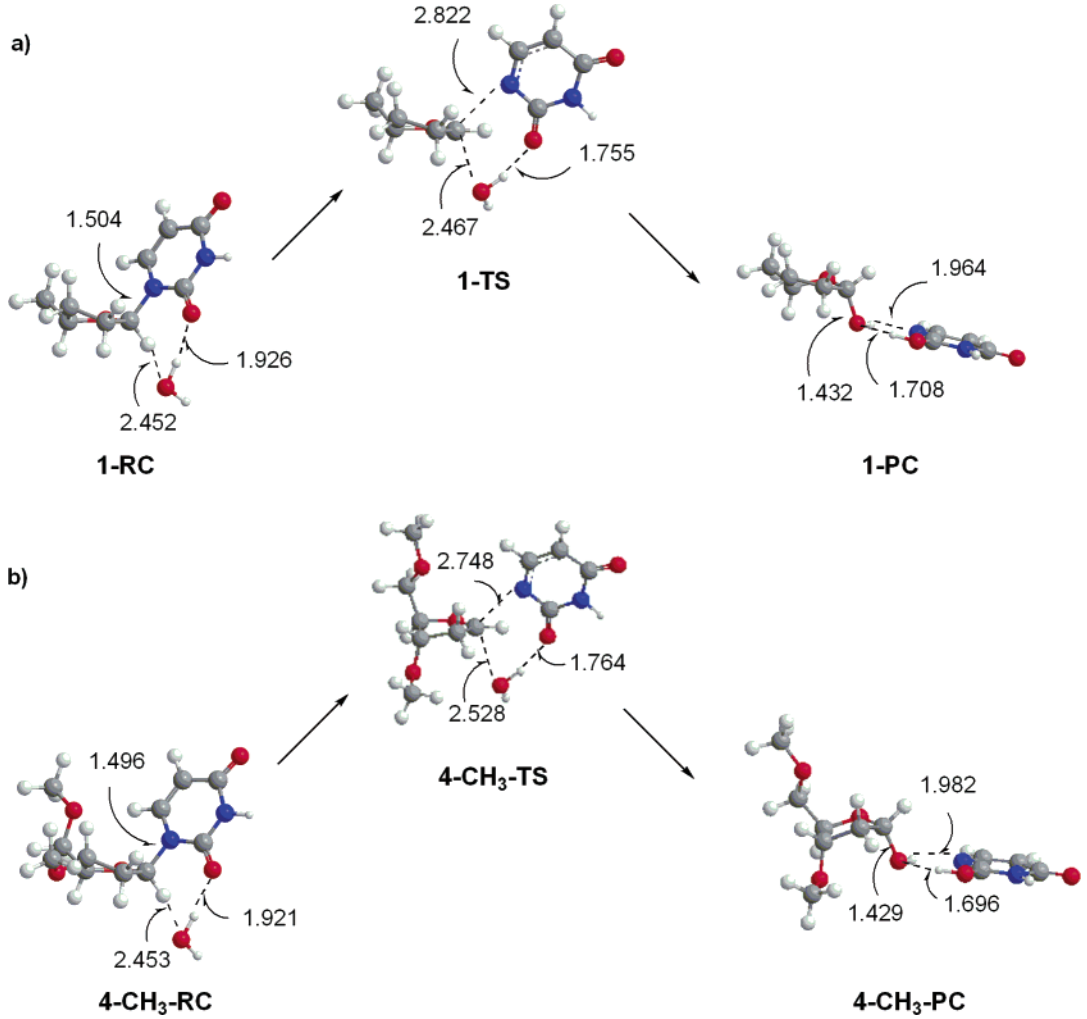

Figure 5. Selected B3LYP/6-31G(d) bond lengths (Å) in reactant (RC), transition state (TS), and product (PC) complexes for the S_N2 pathway for direct hydrolysis of the glycosidic bond in deoxyuridine studied using models (a) **1** and (b) **4-CH$_3$**.

TABLE 2: Barriers and Relative Energies (kJ mol^{-1}) for Direct Hydrolysis of the Glycosidic Bond in Deoxyuridine in Vacuo[a]

S_N1[b]				
model	barrier 1	intermediate energy	barrier 2	reaction energy
1	153.4	81.5	291.6	−1.4
4-CH$_3$	156.8	61.6	272.8	30.7

S_N2[c]		
model	barrier	reaction energy
1	159.7	24.4
4-CH$_3$	165.4	31.2

[a] Relative energies obtained from B3LYP/6-311+G(2d,p) single-point calculations on B3LYP/6-31G(d)-optimized geometries and include scaled (0.9806) ZPVE corrections. [b] See Figure 4. [c] See Figure 5.

the reaction proceeds, uracil abstracts a proton from water, while the remaining hydroxyl anion adds to C1′.

Within active sites of enzymes that use different nucleophiles to catalyze glycosidic bond cleavages, both S_N1 (D_N*A_N)[7,8,39,53] and S_N2 (A_ND_N)[5,6,24,54] reaction paths have been proposed based on transition state analyses. However, the reaction barrier and overall reaction energetics for both mechanisms involving attack at C1′ by water (Table 2) do not differ significantly from those for the unimolecular decomposition in vacuo (Table 1). The large calculated barriers suggest that the role of water as outlined in the above mechanisms is not beneficial to the overall reaction, and therefore the direct involvement of a sole water molecule as a nucleophile is unlikely. This result emphasizes the important catalytic role of enzymes, such as the DNA glycosylases, that facilitate glycosidic bond cleavages in nucleotides.

Role of Activation of the Water Nucleophile on the Reaction Pathway. The results presented in the previous section indicate that a sole water molecule cannot efficiently cleave the glycosidic bond in deoxyuridine. Nevertheless, water has been suggested to play a role in many similar reactions.[5,7−11,15−17,19,24−33] However, it is often proposed that water is initially activated through (at least partial) proton abstraction prior to addition at C1′.[1,2,9−11,17,26] Thus, in the present section, we consider the effects of water activation on the reaction pathway for water-catalyzed glycosidic bond cleavage. Specifically, we interact numerous molecules (Br^-, $HCOO^-$, CN^-, NC^-, F^-, CH_3O^-, and H_2N^-), which have different proton affinities, with water to study the effects of different stages of water activation on the overall mechanism and energetics of glycosidic bond cleavage. We also consider nucleophilic attack by the hydroxyl anion, which represents the extreme of (full) water activation.

The transition structures for glycosidic bond cleavage involving an activated water nucleophile are displayed in Figure 6. The reaction pathways for all activated water models do not involve hydrogen abstraction from the sugar moiety by uracil. This step is no longer required since the sugar cation is stabilized by interactions with both the nucleobase anion and the negatively

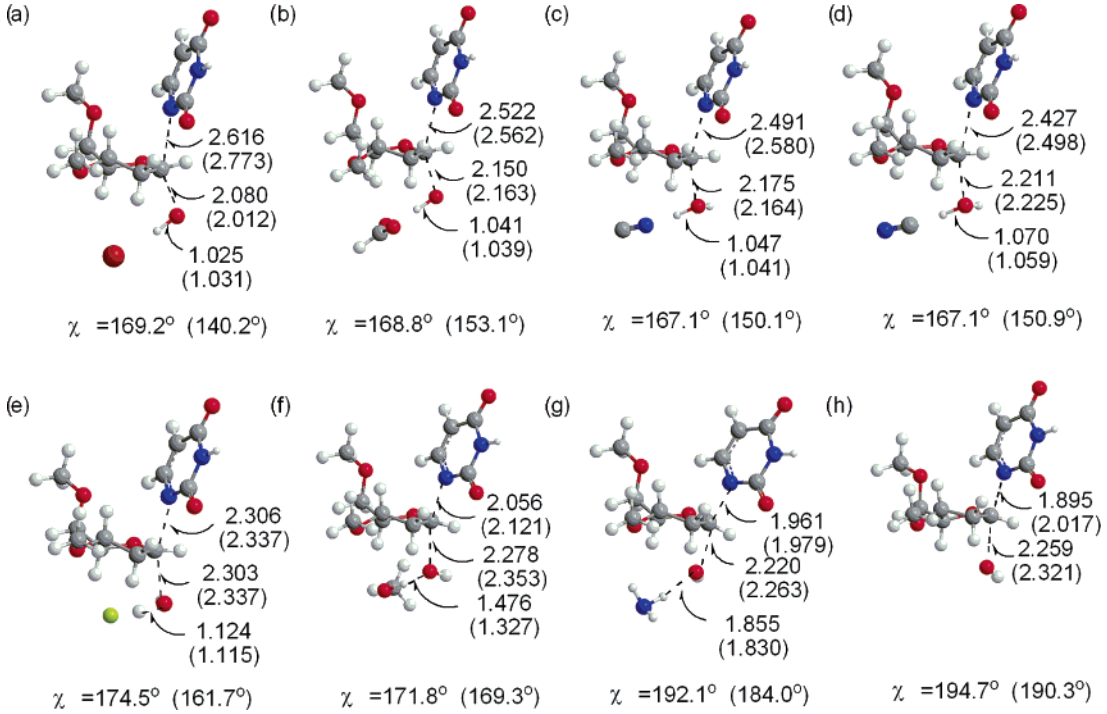

Figure 6. Selected B3LYP/6-31G(d) bond lengths (Å) in transition state complexes for glycosidic bond cleavage involving water activated by (a) Br^-, (b) $HCOO^-$, (c) CN^-, (d) NC^-, (e) F^-, (f) CH_3O^-, and (g) NH_2^- as well as involving (h) the hydroxyl anion (fully activated water) studied using model **4-CH$_3$** (model **1** values in parentheses).

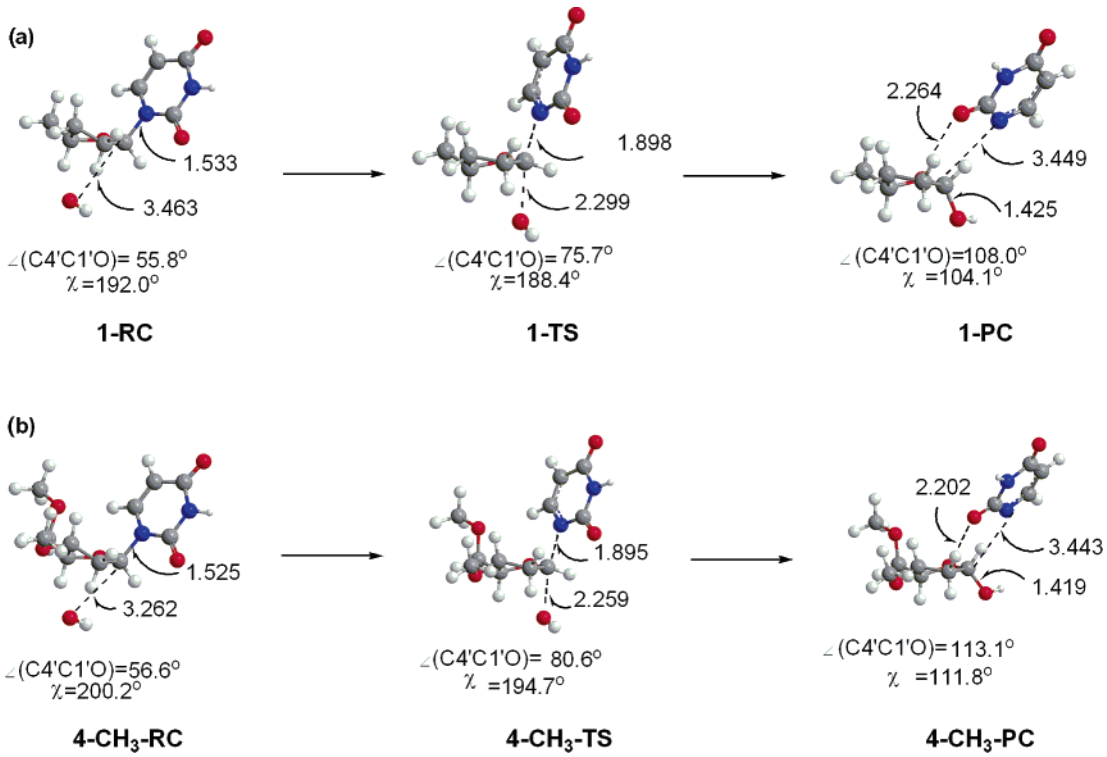

Figure 7. Selected B3LYP/6-31G(d) bond lengths (Å), angles (deg), and dihedral angles (deg) in reactant (RC), transition state (TS), and product (PC) complexes for glycosidic bond cleavage involving a HO^- nucleophile studied using models (a) **1** and (b) **4-CH$_3$**.

charged nucleophile. Indeed, as water activation becomes stronger (i.e., the proton affinity of the molecule interacting with water increases), the interactions with C2′−H are reduced, which can be seen in the increase in the χ ($\angle$(O4′−C1′−N1−C2)) dihedral angle. This is generally accompanied by a steady decrease in the C1′−N1 bond length and an increase in the distance between the water oxygen and C1′. Furthermore, since another molecule activates water, proton abstraction from the water nucleophile by uracil does not occur in these transition structures as discussed previously.

As a representative example of geometrical changes throughout the course of the reaction, we consider hydrolysis by the hydroxyl anion (Figure 7). As the reaction proceeds, the nucleophile swings toward C1′, which increases the C4′−C1′−O_{water} angle, decreases the C1′−O_{water} distance, and lengthens the C1′−N1 bond. In the product complex, the C1′−N1 bond

TABLE 3: Barriers and Reaction Energies (kJ mol^{-1}) for the Glycosidic Bond Cleavage Involving Water, Activated Water, and the Hydroxyl Anion (a Model for the Extreme of (Full) Water Activation (Deprotonation)) Nucleophiles[a,b]

nucleophile	barrier		reaction energy	
H_2O (S_N2)	165.4	(159.7)	31.2	(24.4)
$Br^-\cdots H_2O$	119.3	(107.8)	89.6	(90.0)
$HCOO^-\cdots H_2O$	108.1	(95.9)	15.9	(14.3)
$CN^-\cdots H_2O$	107.9	(97.2)	25.0	(23.5)
$NC^-\cdots H_2O$	106.4	(94.8)	−18.7	(−18.3)
$F^-\cdots H_2O$	84.8	(69.9)	−28.0	(−33.8)
$CH_3O^-\cdots H_2O$	72.9	(60.5)	−79.6	(−83.2)
$H_2N^-\cdots H_2O$	66.4	(59.3)	−116.3	(−121.4)
HO^-	49.9	(49.5)	−163.4	(−161.6)

[a] Model **4-CH$_3$** was used (model **1** values in parentheses). [b] Relative energies obtained from B3LYP/6-311+G(2d,p) single-point calculations on B3LYP/6-31G(d) geometries include scaled (0.9806) ZPVE corrections.

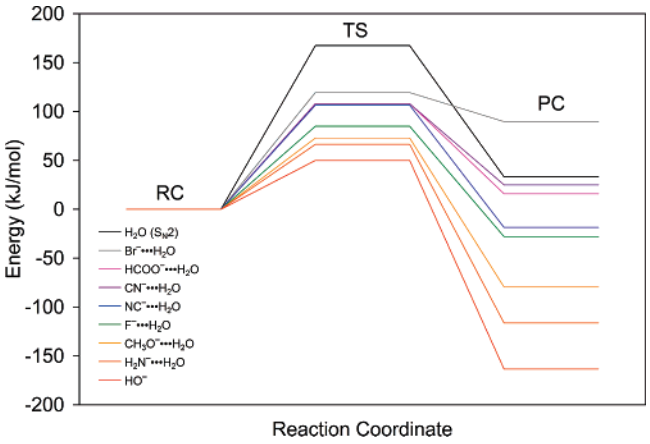

Figure 8. Comparison of B3LYP/6-311+G(2d,p)//B3LYP/6-31G(d) relative barriers and reaction energies for the glycosidic bond cleavage involving water, activated water, and the hydroxyl anion (a model for the extreme of (full) water activation) nucleophiles studied using model **4-CH$_3$**.

is completely cleaved, while the C1′−O$_{water}$ bond is formed. Closer examination of the geometries reveals that there is a significant change in the sugar puckering throughout the reaction, where the reactant complex adopts C3′-endo puckering, the transition structure is in a C3′-endo−C4′-exo twist conformation, and the product adopts C4′-exo puckering. Since the sugar puckering in the transition states of similar reactions has been debated in the literature,[1,10,15,17,31] we performed a series of fixed optimizations, where one dihedral angle between the sugar ring atoms was frozen at zero degrees and the location of the remaining carbon was optimized. We found that the C3′-endo transition structure is the lowest-energy structure compared with C2′-exo (by 3 kJ mol^{-1}), C2′-endo (by 7 kJ mol^{-1}), and C3′-exo (by 9 kJ mol^{-1}). Nevertheless, the C3′-endo conformation optimizes to the lower-energy C3′-endo−C4′-exo twist structure when the constraint is released.

The energetics for the reactions involving activated water are summarized in Table 3. The activating molecules lead to a steady decrease in the reaction barrier and an increase in the exothermicity of the overall reaction, as the proton affinity of the molecule interacting with water increases. This trend can be clearly seen in Figure 8 for model **4-CH$_3$**. Our calculations suggest that attack at C1′ by the hydroxyl anion leads to the smallest (50 kJ mol^{-1}) barrier and largest exothermicity (−160 kJ mol^{-1}), which is likely due to the stabilization provided by the hydroxyl anion to the sugar cation formed upon glycosidic bond cleavage. Indeed, it has been proposed that stabilization

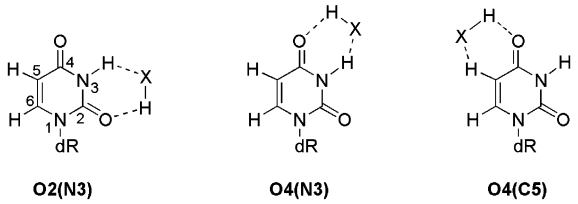

Figure 9. Complexes between deoxyuridine and small molecules (XH = HF, H_2O, and NH_3) investigated in the present study.

of the oxocarbenium sugar cation has a significant effect on the kinetics of glycosidic bond cleavages.[1,2] We note that the barriers as well as reaction energies calculated using models **1** and **4-CH$_3$** differ more significantly for these reactions compared with the differences discussed for the unimolecular decomposition or direct hydrolysis due to repulsive interactions between the molecule activating water and O3′ in model **4-CH$_3$**.

In summary, we find that the barrier heights for glycosidic bond cleavage range from that discussed for water (S_N2) to that corresponding to full water activation (HO^- nucleophile) when different molecules are used to partially activate water via hydrogen bonding. This finding, in conjunction with the high barrier found for direct cleavage by water, stresses the important role of water activation in the cleavage of the glycosidic bond in deoxyuridine.

Role of Hydrogen Bonding with the Nucleobase on the Reaction Pathway. Many enzymes that catalyze glycosidic bond cleavage have been proposed to lower reaction barriers via hydrogen bonding between substrates and active site amino acid residues.[1,2,9−11,14,18,21,22,26,27,29,31−34,37,38] Therefore, it is of interest to consider the effects of hydrogen bonding with the nucleobase on the reaction profile for the glycosidic bond cleavage in deoxyuridine. Previous work in our group has considered the effects of hydrogen bonds on the N1 acidity of uracil by binding three small molecules (HF, H_2O, and NH_3), which have a range in acidity and proton affinity, at three nucleobase sites (denoted as O2(N3), O4(N3), and O4(C5) (Figure 9)).[42] The effect of hydrogen bonding on the acidity of uracil was considered due to the proposed formation of the uracil anion during glycosidic bond cleavage catalyzed by uracil DNA glycosylase, a DNA repair enzyme.[1,2] We can complement our previous work by considering the effects of these hydrogen bonds on the kinetics and thermodynamics of this important reaction.

Initially, the effects of hydrogen bonds on the barrier and the reaction energy for the hydrolysis of the glycosidic bond in deoxyuridine by the hydroxyl anion were considered, which mimics the extreme of (full) water activation (deprotonation). Although we focus our discussion on model **4-CH$_3$** (Table 4), similar results were obtained with model **1** (Supporting Information, Table S4). Although ammonia slightly increases the barrier when bound to O2(N3) or O4(N3), complexation of a small molecule to various sites in uracil generally reduces the energy barrier and makes the reaction more exothermic (see Δ(barrier) and Δ(energy), Table 4, where a negative value corresponds to a decrease in the barrier or reaction energy). Specifically, the barrier drops by 10−13 kJ mol^{-1} for HF, 4−7 kJ mol^{-1} for H_2O, and 4 kJ mol^{-1} for NH_3. This trend corresponds to the properties of the small molecules, where the magnitude of the effect increases with the acidity of the small molecule bound. There is also a clear trend in the effect of the complexation site. Specifically, complexation at O2(N3) leads to the largest decrease in the barrier when HF is bound to uracil, while complexation at O4(C5) leads to the largest decrease for H_2O and NH_3. O4(N3) leads to the smallest decrease for all three

TABLE 4: Barriers and Reaction Energies (kJ mol^{-1}) for Hydrolysis of the Glycosidic Bond in Deoxyuridine by HO$^-$ for Model 4-CH$_3$ with HF, H$_2$O, or NH$_3$ Bound at Various Sites in Uracil as well as Binding Strengths for Uracil, Uracil (N1) Anion, and the Reactant, Transition State, and Product Complexes[a,b]

								binding strength					differences in binding strengths		
O2(N3)	O4(N3)	O4(C5)	barrier	Δ(barrier)	reaction energy	Δ(energy)	Δ(acidity)[c,d]	U[d]	U$^-$ [d]	RC	TS	PC	Δ(RC−U)	Δ(TS−U$^-$)	Δ(PC−U$^-$)
			49.9	0.0	−163.4	0.0	0.0								
HF			37.2	−12.7	−188.6	−25.2	51.5	35.6	87.1	50.2	62.9	75.3	14.6	−24.2	−11.8
	HF		40.2	−9.7	−182.8	−19.4	42.7	40.1	82.8	54.4	64.0	73.7	14.3	−18.8	−9.1
		HF	38.5	−11.4	−185.1	−21.7	46.9	37.3	84.2	52.7	64.0	74.2	15.4	−20.2	−10.0
H$_2$O			44.4	−5.5	−174.5	−11.1	20.2	22.4	42.6	22.9	28.4	33.9	0.5	−14.2	−8.7
	H$_2$O		45.9	−4.0	−172.0	−8.6	15.7	24.9	40.6	23.9	27.9	32.4	−1.0	−12.7	−8.2
		H$_2$O	43.1	−6.8	−176.2	−12.8	13.0	29.5	42.5	21.9	28.7	34.6	−7.6	−13.8	−7.9
NH$_3$			51.0	1.1	−162.8	0.6	−3.2	22.5	19.3	13.6	12.4	12.9	−8.9	−6.9	−6.4
	NH$_3$		51.8	1.9	−162.7	0.7	−5.3	23.4	18.1	13.0	11.0	12.1	−10.4	−7.1	−6.0
		NH$_3$	45.7	−4.2	−171.7	−8.3	9.1	10.2	19.3	8.3	12.5	16.5	−1.9	−6.8	−2.8

[a] B3LYP/6-311+G(2d,p) single-point calculations were performed on B3LYP/6-31G(d) geometries and include scaled (0.9806) ZPVE corrections. [b] See Figure 9 for definition of complexation sites. [c] Acidity of uracil calculated at the same level of theory is 1389.5 kJ mol^{-1}. [d] Reference 42.

TABLE 5: Model 4-CH$_3$ Barriers and Reaction Energies (kJ mol^{-1}) for Hydrolysis of the Glycosidic Bond in Deoxyuridine by HO$^-$ or Water Activated by CH$_3$O$^-$ or HCOO$^-$ with HF, H$_2$O, or NH$_3$ Bound at Various Sites in Uracil[a,b]

			HO$^-$				CH$_3$O$^-$···H$_2$O				HCOO$^-$···H$_2$O			
O2(N3)	O4(N3)	O4(C5)	barrier	Δ	reaction energy	Δ	barrier	Δ	reaction energy	Δ	barrier	Δ	reaction energy	Δ
			49.9	0.0	−163.4	0.0	72.9	0.0	−79.6	0.0	108.1	0.0	15.9	0.0
HF			37.2	−12.7	−188.6	−25.2	57.1	−15.8	−106.4	−26.8	87.3	−20.8	−11.0	−26.9
	HF		40.2	−9.7	−182.8	−19.4	61.5	−11.4	−98.4	−18.8	92.3	−15.8	−8.5	−24.4
		HF	38.5	−11.4	−185.1	−21.7	59.6	−13.3	−100.4	−20.8	89.8	−18.3	−6.6	−22.5
H$_2$O			44.4	−5.5	−174.5	−11.1	68.1	−4.8	−88.8	−9.2	100.7	−7.4	5.4	−10.5
	H$_2$O		45.9	−4.0	−172.0	−8.6	69.2	−3.7	−86.9	−7.3	101.8	−6.3	6.7	−9.2
		H$_2$O	43.1	−6.8	−176.2	−12.8	65.6	−7.3	−91.8	−12.2	97.8	−10.3	3.2	−12.7
NH$_3$			51.0	1.1	−162.8	0.6	76.6	3.7	−76.5	3.1	111.1	3.0	16.4	0.5
	NH$_3$		51.8	1.9	−162.7	0.7	76.8	3.9	−76.4	3.2	110.5	2.4	17.3	1.4
		NH$_3$	45.7	−4.2	−171.7	−8.3	69.3	−3.6	−86.8	−7.2	102.6	−5.5	8.5	−7.4

[a] B3LYP/6-311+G(2d,p) single-point calculations were performed on the 6-31G(d) geometries. Scaled (0.9806) ZPVE corrections are included in all energies. [b] See Figure 9 for definition of complexation sites.

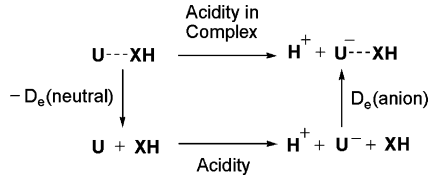

Figure 10. Thermodynamic cycle for the deprotonation of uracil (U) hydrogen-bonded to another molecule (XH).

small molecules. The reaction energy follows the same trends as the reaction barrier, where the biggest effect (−25.2 kJ mol^{-1}) is seen when HF is bound at O2(N3).

The trends found in the present work with respect to the small molecule and binding site are similar to those previously reported for the (N1) acidity of uracil (Δ(acidity), Table 4).[42] However, the magnitude of the effect on the acidity was found to be up to 50 kJ mol^{-1}, which is approximately 4 times larger than the maximum (13 kJ mol^{-1}) effect on the barrier and double the maximum (25 kJ mol^{-1}) effect on the reaction energy. The differences between the effect of hydrogen bonding on the acidity and the barriers or reaction energy can be understood by considering the binding strengths of the small molecules to uracil. Specifically, in our previous work, we identified that the effect of hydrogen bonding on the acidity of uracil arises due to stronger binding of the small molecule to the uracil anion compared with that to uracil and that the effect is equal to the difference between the two binding strengths as shown using a simple thermodynamic cycle (Figure 10).[42] For example, the binding strength of HF to O2(N3) in uracil is 35.6 kJ mol^{-1}, but the binding to the uracil anion is 87.1 kJ mol^{-1}. Therefore, the acidity increases by 51.5 kJ mol^{-1} (Table 4).

Similarly, the effects of hydrogen bonding on the reaction energy (barrier) can be defined as the difference between the binding strengths within the reactant and product (transition state) complexes. Thus, to understand the differences in the effects on the acidity and the reaction energy (barrier), we must compare the binding strengths of uracil and the reactant complex as well as the binding strengths of the uracil anion and the product (transition state) complex. For example, if binding is stronger to the reactant complex than uracil, then the effect of hydrogen bonding on the reaction energy (barrier) will be less than the effect on the acidity. Alternatively, if binding is stronger to the product (transition state) complex than the uracil anion, then the effect of hydrogen bonding on the reaction energy (barrier) will be greater than the effect on the acidity.

The binding strengths of the small molecule to the nucleobase and differences in the binding strengths are included in Table 4. We find that hydrogen fluoride binds stronger to the reactant complex than uracil (Δ(RC−U) > 0), but binds weaker to the product and transition state complexes than the uracil anion (Δ(TS−U$^-$) and Δ(PC−U$^-$) < 0). Both differences lead to smaller effects of the small molecule, and therefore the effects of hydrogen bonding on the reaction energy and barrier are much smaller than the effect on the acidity. Furthermore, the binding strength in the transition state complex is less than that in the product complex, and therefore the difference between the effect

on the acidity and the barrier is larger than the difference for the reaction energy.

Similar arguments can be used to understand the difference in the effects of interactions with water and ammonia. For example, the binding strengths of water to the reactant complex and uracil are similar, but binding to the product complex is weaker than that to the uracil anion, and binding to the transition state is weaker than that to the product complex. Therefore, the effect on the acidity is greater than that on the reaction energy, which is greater than the effect on the barrier. Ammonia, however, binds weaker to the reactant complex than to uracil and binds weaker to the product and transition state complexes than to the uracil anion. Since the magnitudes of these differences are almost equal, the effects on the acidity, barrier, and reaction energy are almost the same.

The decrease in the effect of hydrogen bonding as acidity > reaction energy > barrier correlates with a decrease in the charge on the nucleobase. However, the magnitude of the difference is surprising. Therefore, to expand our study, we compare the effects of hydrogen-bonding interactions with the nucleobase on the hydrolysis of the glycosidic bond in deoxyuridine by the hydroxyl anion (the extreme case of (full) water activation) to the corresponding effects when the nucleophile is water activated by the methoxyl anion ($CH_3O^-\cdots H_2O$) or the formate anion ($HCOO^-\cdots H_2O$). (Table 5 contains data for model **4-CH$_3$**, while Table S5 (Supporting Information) contains the data for model **1**.) These models were chosen to span the range of barriers found, where the barriers without hydrogen-bonding interactions are approximately 50 kJ mol^{-1} for HO^-, 75 kJ mol^{-1} for $CH_3O^-\cdots H_2O$, and 110 kJ mol^{-1} for $HCOO^-\cdots H_2O$.

The magnitude of the effect of hydrogen bonding on the reaction energy is similar for all reactions (Table 5). This likely occurs since the uracil anion receives similar stabilization from the sugar moiety in all models. However, the effect on the barrier is larger for the reaction involving $HCOO^-$-activated water as the nucleophile than the reaction involving CH_3O^--activated water, which is larger than that for the reaction involving the hydroxyl anion. These changes in the effect of hydrogen bonding on the barrier are expected since the C1′−N1 bond in the transition state increases with a decrease in the proton affinity of the molecule activating water (Figure 6). Specifically, this implies that the activated water reaction paths have later transition states or that the nucleobase in the transition state has a greater negative charge as the proton affinity of the molecule activating water decreases. Therefore, the nucleobase is stabilized to a greater extent through hydrogen bonding with the small molecules in the transition state. Indeed, as the proton affinity of the molecule activating water decreases, the effects on the barrier and the reaction energy become more similar in magnitude. We note that similar (although slightly smaller) reductions in the barriers were found for direct hydrolysis by water (S_N2); however, the resulting barriers are still too large to consider this as a feasible pathway, and therefore the results are not further discussed.

Despite differences in the effects of hydrogen bonding, the barriers increase as $HO^- < CH_3O^-\cdots H_2O < HCOO^-\cdots H_2O$ regardless of the small molecule bound or the binding site. Therefore, it can be concluded that the effect of the nucleophile on the reaction barrier is much greater than the effect of hydrogen bonding with HF, H_2O, or NH_3. Furthermore, the effects of hydrogen bonding on the barrier and reaction energy for the reactions involving CH_3O^-- or $HCOO^-$-activated water and the hydroxyl anion follow the same trends with respect to

TABLE 6: Comparison of the Barriers and Reaction Energies (kJ mol^{-1}) for Hydrolysis of the Glycosidic Bond in Deoxyuridine by HO$^-$ or HCOO$^-$-Activated Water Calculated with a Variety of Density Functional Methods[a,b]

				B3LYP[c]			MPW1B95[d]			MPWB1K[d]			PWB6K[d]		
nucleophile	O2(N3)	O4(N3)	O4(C5)	barrier	Δ	reaction energy	Δ	barrier	Δ	reaction energy	Δ	barrier	Δ	reaction energy	Δ	barrier	Δ	reaction energy	Δ
HO^-				49.9		−163.4		55.8		−155.5		61.0		−160.3		62.1		−161.1	
	HF			37.2	−12.7	−188.6	−25.2	43.2	−12.6	−180.6	−25.1	48.2	−12.8	−185.6	−25.3	47.6	−14.5	−189.2	−28.1
		HF		40.2	−9.7	−182.8	−19.4	46.0	−9.8	−174.8	−19.3	51.0	−10.0	−180.0	−19.7	50.3	−11.8	−183.7	−22.6
			HF	38.5	−11.4	−185.1	−21.7	44.4	−11.4	−177.1	−21.6	49.5	−11.5	−182.1	−21.8	48.8	−13.3	−185.3	−24.2
	H_2O			44.4	−5.5	−174.5	−11.1	50.2	−5.5	−168.7	−13.2	55.6	−5.4	−171.0	−10.7	55.0	−7.1	−174.3	−13.2
		H_2O		45.9	−4.0	−172.0	−8.6	51.6	−4.2	−166.9	−11.4	56.9	−4.1	−169.6	−9.3	56.2	−5.9	−172.9	−11.8
			H_2O	43.1	−6.8	−176.2	−12.8	49.0	−6.8	−170.5	−15.0	54.3	−6.8	−175.4	−15.1	53.6	−8.5	−176.2	−15.1
	NH_3			51.0	1.1	−162.8	0.6	56.9	1.1	−156.1	−0.6	62.6	1.5	−159.2	1.1	61.9	−0.2	−161.7	−0.6
		NH_3		51.8	1.9	−162.7	0.7	57.5	1.8	−154.7	0.8	63.1	2.1	−159.5	0.8	62.5	0.4	−162.0	−0.9
			NH_3	45.7	−4.2	−171.7	−8.3	52.2	−3.6	−163.9	−8.4	57.7	−3.3	−168.7	−8.4	57.1	−5.0	−169.3	−8.2
$HCOO^-\cdots H_2O$				108.1		15.9		125.4		24.6		135.4		25.9		135.0		27.3	
	HF			87.3	−20.8	−11.0	−26.9	105.6	−19.8	−1.1	−25.7	115.3	−20.1	0.0	−25.9	114.8	−20.3	1.0	−26.3
		HF		92.3	−15.8	−8.5	−24.4	109.7	−15.7	4.7	−19.9	119.4	−16.0	6.3	−19.6	118.8	−16.2	7.9	−19.4
			HF	89.8	−18.3	−6.6	−22.5	107.3	−18.1	2.8	−21.8	116.9	−18.5	4.0	−21.9	116.4	−18.7	5.4	−21.9
	H2O			100.7	−7.4	5.4	−10.5	118.2	−7.2	14.2	−10.4	128.2	−7.2	15.6	−10.3	128.8	−6.2	16.9	−10.4
		H2O		101.8	−6.3	6.7	−9.2	118.9	−6.5	15.3	−9.3	128.7	−6.7	16.6	−9.3	127.2	−7.9	18.0	−9.3
			H2O	97.8	−10.3	3.2	−12.7	113.3	−12.1	12.2	−12.4	122.7	−12.7	13.4	−12.5	121.9	−13.2	14.8	−12.5
	NH3			111.1	3.0	16.4	0.5	128.5	3.1	25.7	1.1	138.6	3.2	27.1	1.2	138.2	3.1	28.2	0.9
		NH3		110.5	2.4	17.3	1.4	127.5	2.1	25.7	1.1	137.6	2.2	27.1	1.2	137.2	2.2	28.4	1.1
			NH3	102.6	−5.5	8.5	−7.4	120.1	−5.3	18.2	−6.4	130.1	−5.3	19.7	−6.2	129.8	−5.2	21.4	−5.9

[a] See Figure 9 for definition of complexation sites. [b] All relative energies were obtained from single-point calculations on B3LYP/6-31G(d) geometries and include ZPVE and BSSE corrections. B3LYP/6-311+G(2d,p) BSSE corrections were used for all functionals due to the similarity in the values calculated for a subset of the reactions. [c] The 6-311+G(2d,p) basis set was used. [d] The 6-311+G(2df,2p) basis set was used.

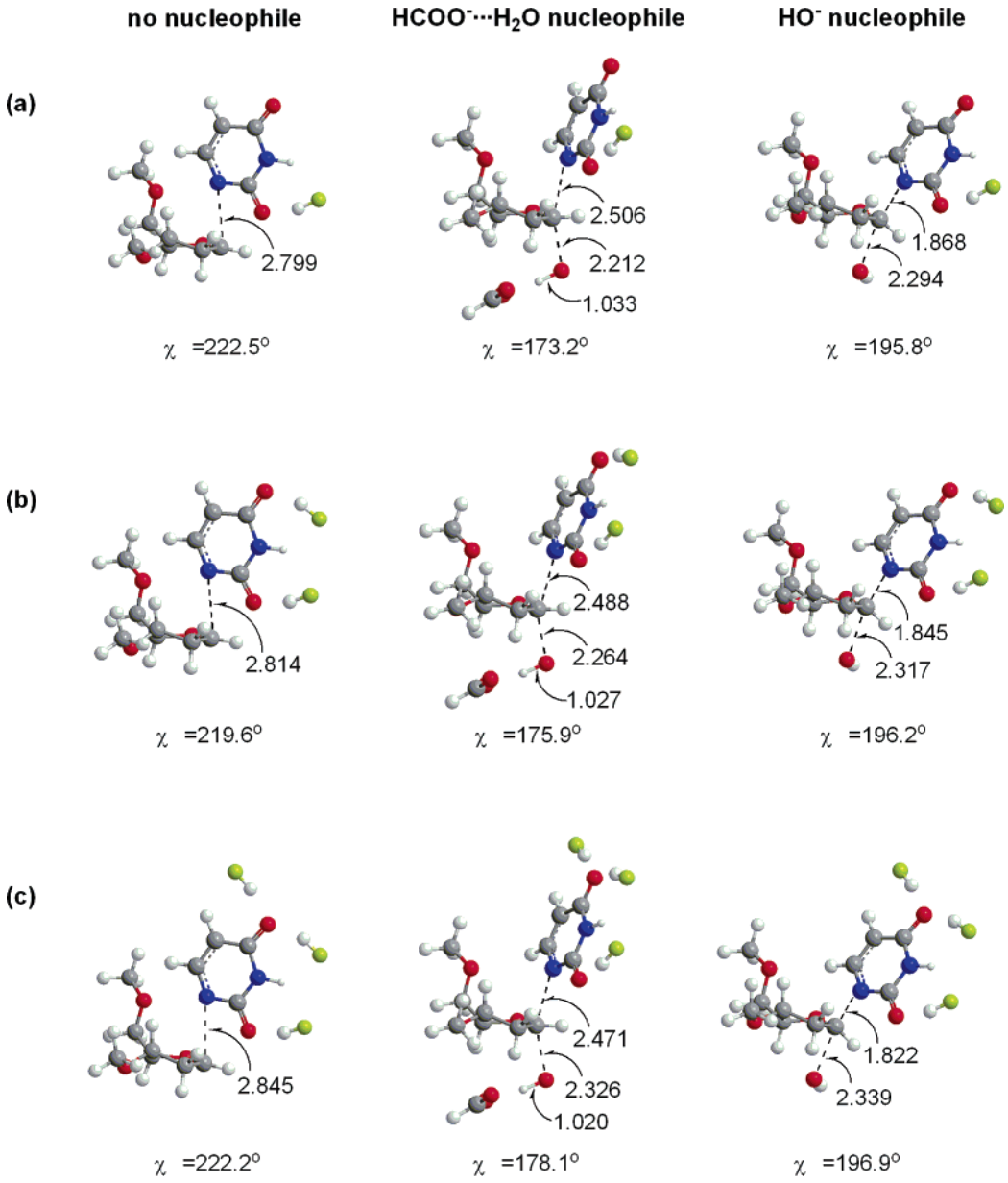

Figure 11. Representative examples of transition structures for glycosidic bond cleavage in deoxyuridine when (a) one, (b) two, and (c) three hydrogen fluoride molecules are bound to the nucleobase and a variety of nucleophiles are considered.

the small molecule (i.e., the effects are largest when HF is bound to O2(N3) or when H_2O or NH_3 is bound to O4(C5)).

The popular B3LYP hybrid density functional,[44] which consists of 20% exchange, accurately predicts thermochemical properties[55] but systematically underestimates barrier heights.[56,57] Although B3LYP has been used to study related glycosidic bond cleavage reactions,[22,35] we compare a subset of our results to other hybrid density functionals. Specifically, it has been shown that more accurate kinetic results can be obtained by increasing the fraction of Hartree−Fock exchange[58] in the hybrid density functional theory.[59] As a result, Truhlar and co-workers have introduced a number of density functional methods for the calculation of accurate thermochemical kinetics data.[60,61,62,63] We have chosen to compare our B3LYP results with three of these functionals: MPWB1K, MPW1B95, and PWB6K.[64] Truhlar recommends MPW1B95 for general purpose applications and all three of these functionals for kinetics studies.

The MPW1B95, MPWB1K, and PWB6K barriers and reaction energies for hydrolysis by the HO^- and $HCOO^-\cdots H_2O$ nucleophiles are displayed in Table 6. As anticipated, newer density functionals predict larger barriers than B3LYP by up to 12 kJ mol^{-1} for the HO^- and 28 kJ mol^{-1} for the $HCOO^-\cdots H_2O$ nucleophile. Nevertheless, the effects of hydrogen-bonding interactions between small molecules and the nucleobase on the barriers and reaction energies are preserved by all functionals. For example, deviations in the effects of hydrogen bonds on the barrier predicted by B3LYP are generally less than 1 kJ mol^{-1} for MPW1B95 and MPWB1K and less than 3 kJ mol^{-1} for PWB6K. The relative magnitude of the effect of XH on the barrier and reaction energies with the HO^- and $HCOO^-\cdots H_2O$ nucleophiles are also similar among all functionals, which suggests that the effects of changing the nucleophile are also preserved.

In summary, our calculations indicate that hydrogen-bonding interactions between small molecules and uracil can decrease the barrier for the hydrolysis of the glycosidic bond in deoxyuridine by the hydroxyl anion (the extreme of (full) water activation). However, the decrease in the barrier and reaction energy is smaller than the corresponding increase in the acidity, which can be understood by considering the binding strengths

TABLE 7: Comparison of Barriers and Reaction Energies (kJ mol^{-1}) Calculated for a Variety of Nucleophiles when the Nucleobase Is Stabilized through Interactions with Multiple Hydrogen Fluoride Molecules[a-c]

			no nucleophile		$HCOO^-\cdots H_2O$		HO^-	
O2(N3)	O4(N3)	O4(C5)	barrier	reaction energy	barrier	reaction energy	barrier	reaction energy
HF			179.4	57.7	87.3	−11.0	37.2	−188.6
	HF		175.8	69.8	92.3	−8.5	40.2	−182.8
		HF	175.8	75.0	89.8	−6.6	38.5	−185.1
HF	HF		174.0	99.9	73.0	−29.2	29.5	−206.0
HF		HF	166.7	96.4	70.8	−31.6	27.6	−208.2
	HF	HF	165.5	69.6	77.4	−22.8	31.8	−199.7
HF	HF	HF	156.4	91.0	60.1	−46.2	22.4	−221.0

[a] B3LYP/6-311+G(2d,p) relative energies were calculated on B3LYP/6-31G(d) geometries for model **4-CH$_3$** and include ZPVE and BSSE corrections. [b] See Figure 9 for definition of complexation sites. [c] See Figure 11 for pictures of representative transition states.

of the appropriate complexes. Effects of hydrogen bonds on the reaction profile are found to increase for catalysis by HO^- < $CH_3O^-\cdots H_2O$ < $HCOO^-\cdots H_2O$, but the corresponding barriers also increase along the same trend. Since the trends (with respect to the molecule bound and the binding site) are the same for all reaction pathways, future studies on other nucleosides can consider the hydrolysis of the glycosidic bond in nucleosides by the hydroxyl anion and the nucleobase acidity to determine the minimum and maximum effects of hydrogen-bonding interactions with the nucleobase on the reaction profile.

Role of the Nucleophile on the Reaction Pathway. The previous section has shown that activation of the nucleobase can play an important role in lowering the barrier for hydrolysis of the glycosidic bond by activated water. Although it is also intriguing to analogously determine the role of the nucleophile on the reaction pathway, our previous models without a nucleophile, which described the unimolecular decomposition of deoxyuridine in vacuo, are not realistic models since the instability of charge-separated species in the gas phase leads to unrealistic products (for example, abstraction of C2′−H). A better estimate of the effects of the nucleophile can be obtained by considering models where the nucleobase is stabilized by hydrogen-bonding interactions with small molecules. Indeed, we have isolated transition states for the glycosidic bond cleavage in deoxyuridine in the absence of a nucleophile when one to three hydrogen fluoride molecules are bound to the nucleobase (Figure 11). Comparison of the energetics for these pathways to the corresponding reactions when the HO^- and $HCOO^-\cdots H_2O$ nucleophiles are present will better allow us to determine the effect of the nucleophile.

Although the decrease in the barrier height upon inclusion of the nucleophiles does not follow a clear trend with an increase in the number of small molecules bound to the nucleobase (Table 7), inclusion of the $HCOO^-\cdots H_2O$ nucleophile in the reaction decreases the barrier to glycosidic bond cleavage by 83−101 kJ mol^{-1}. Additionally, inclusion of HO^-, a stronger nucleophile, leads to larger decreases (183−221 kJ mol^{-1}) in the barrier to glycosidic bond cleavage. These results reemphasize the important role of the nucleophile in the glycosidic bond cleavage reaction. Furthermore, the greater decreases in the barriers upon inclusion of the HO^- nucleophile compared with $HCOO^-\cdots H_2O$ reemphasize the important role of (increased) nucleophile activation.

Since a greater number of small molecules were bound to the nucleobase, the synergy of simultaneous interactions with the nucleobase can now be evaluated. Specifically, we have been interested in the additivity of the effects of multiple interactions with the nucleobase.[42] Using the data without hydrogen fluoride bound (Table 5), we can compare the calculated (simultaneous) effect of more than one HF on the barrier for glycosidic bond cleavage to the sum of the individual (additive) effects when the $HCOO^-\cdots H_2O$ and HO^- nucleophiles are present (Table 7). We find that when one HF is bound at O2(N3) and another is bound at either O4 site the simultaneous effects are within 2 kJ mol^{-1} of the sum of the individual (additive) effects for both nucleophiles. When HF is bound at both O4 sites, the calculated effects are less than additive by 3 kJ mol^{-1}. These results suggest that interactions between the nucleobase and more than one amino acid residue within the active sites of enzymes that facilitate glycosidic bond cleavages will be beneficial to the overall reaction. However, larger (6−7 kJ mol^{-1}) deviations from additivity are seen when three hydrogen fluorides are simultaneously bound to uracil, which suggests that there is a limit to the net stabilization provided to the nucleobase as the number of hydrogen bonds increases. Nevertheless, the effects of three HF molecules is at least 5 kJ mol^{-1} greater than the effects of two HF molecules bound at any combination of sites. Therefore, there are still benefits when more than two interactions simultaneously work together to facilitate these difficult bond cleavage reactions. These results may help explain why so many nucleobase sites are involved in close contacts with amino acids within the active sites of enzymes that catalyze glycosidic bond cleavage reactions.

Conclusions

Glycosidic bonds are cleaved during a number of important biological processes, including DNA repair and nucleotide salvage pathways. All proposed mechanisms for these reactions involve (at least partial) formation of a sugar cation and/or base anion, activation of the nucleophile, and/or stabilization of the nucleobase anion by hydrogen-bonding interactions with active site residues. The present study uses computational chemistry to study these aspects of the kinetics and thermodynamics of the glycosidic bond cleavage in the smallest nucleotide, deoxyuridine.

The most favorable route for the unimolecular glycosidic bond cleavage in deoxyuridine in vacuo was determined to involve abstraction of a (C2′) sugar hydrogen by uracil. This reaction pathway is associated with a large barrier and an endothermic enthalpy, and there is no experimental evidence to support the formation of a ribal intermediate. Therefore, since water is present in the active site of many enzymes and it has been proposed that water is involved in many glycosidic bond cleavage pathways, we subsequently considered direct hydrolysis of the glycosidic bond. Two reaction pathways were characterized, which involve significant activation energies and endothermic reaction energies, and therefore our results suggest that a sole water molecule is not sufficient for glycosidic bond cleavage. However, it was previously proposed that amino acid residues activate nucleophiles involved in glycosidic bond cleavage processes, and thus we considered partial activation

of water. We found that the barriers for these reactions range between that for water catalysis and that for catalysis by the hydroxyl anion, which represents the extreme of (full) water activation (deprotonation).

The glycosidic bond cleavage reaction was further considered by characterizing the effects of hydrogen-bonding interactions with the nucleobase. The effects of the hydrogen-bonding interactions on the barrier and reaction energy were found to be larger for reactions catalyzed by partially activated water compared with the hydroxyl anion but smaller than the effects on the nucleobase acidity. Regardless of these differences, our results provide estimates of the minimum and maximum effects of hydrogen-bonding interactions with the nucleobase on the reaction energetics and emphasize the importance of hydrogen-bonding interactions with the nucleobase on the reaction energetics. Furthermore, consideration of model systems with the nucleobase involved in hydrogen bonds with multiple hydrogen fluoride molecules reemphasizes the important role of the nucleophile in the catalysis of the glycosidic bond cleavage in deoxyuridine and led to suggestions that two or more hydrogen-bonding interactions with the nucleobase can work together to facilitate the bond cleavage.

In summary, the present work considers some fundamental aspects of an important biological reaction that is catalyzed by many different enzymes. Therefore, our results will have general implications for many biological processes. We are currently considering the effects of solvation on the reaction profile as well as similar reactions for other nucleotides.

Acknowledgment. We thank the Research Corporation, the Natural Sciences and Engineering Research Council of Canada, the Canada Foundation for Innovation, and the New Brunswick Innovation Foundation for financial support. We also gratefully acknowledge the Mount Allison Cluster for Advanced Research for generous allocations of computer resources. We thank an anonymous referee for useful comments that have strengthened our discussion.

Supporting Information Available: Selected B3LYP/6-31G(d) and B3LYP/6-31+G(d,p) geometrical parameters for the unimolecular decomposition of deoxyuridine and the glycosidic bond cleavage facilitated by HO^-, comparison of the barriers and reaction energies calculated using the B3LYP/6-31G(d) and B3LYP/6-31+G(d,p) geometries for the unimolecular decomposition, direct hydrolysis of the glycosidic bond, and hydrolysis by the HO^- nucleophile, comparison of barriers and reaction energies calculated with the B3LYP/6-31G(d) and B3LYP/6-31+G(d,p) geometries for hydrolysis by the HO^- nucleophile with small molecules complexed to the nucleobase using model **1**, and barriers and reaction energies calculated with B3LYP/6-31G(d) geometries and model **1** for hydrolysis by activated water when small molecules are bound to the nucleobases. This material is available free of charge via the Internet at http://pubs.acs.org.

References and Notes

(1) Stivers, J. T.; Jiang, Y. L. *Chem. Rev.* **2003**, *103*, 2729−2759.

(2) Berti, P. J.; McCann, J. A. B. *Chem. Rev.* **2006**, *106*, 506−555.

(3) (a) David, S. S.; Williams, S. D. *Chem. Rev.* **1998**, *98*, 1221−1261. (b) Stivers, J. T.; Drohat, A. C. *Arch. Biochem. Biophys.* **2001**, *396*, 1−9. (c) Boiteux, S.; Gellon, L.; Guibourt, N. *Free Radical Biol. Med.* **2002**, *32*, 1244−1253. (d) Vasilenko, N. L.; Nevinsky, G. A. *Mol. Biol.* **2003**, *37*, 803−817.(e) Barnes, D. E.; Lindahl, T. *Annu. Rev. Genet.* **2004**, *38*, 445−476. (f) Huffman, J. L.; Sundheim, O.; Tainer, J. A. *Mutat. Res.* **2005**, *577*, 55−76.

(4) Voet, D.; Pratt, C. W.; Voet, J. G. *Fundamentals of Biochemistry, Upgrade Edition*; Wiley: New York, 2002.

(5) (a) Mentch, F.; Parkin, D. W.; Schramm, V. L. *Biochemistry* **1987**, *26*, 921−930.; (b) Berti, P. J.; Schramm, V. L. *J. Am. Chem. Soc.* **1997**, *119*, 12069−12078.

(6) Kline, P. C.; Schramm, V. L. *Biochemistry* **1995**, *34*, 1153−1162.

(7) (a) Chen, X.-Y.; Berti, P. J.; Schramm, V. L. *J. Am. Chem. Soc.* **2000**, *122*, 1609−1617. (b) Chen, X.-Y.; Berti, P. J.; Schramm, V. L. *J. Am. Chem. Soc.* **2000**, *122*, 6527−6534.

(8) Werner, R. M.; Stivers, J. T. *Biochemistry* **2000**, *39*, 14054−14064.

(9) Mazumder, D.; Kahn, K.; Bruice, T. C. *J. Am. Chem. Soc.* **2002**, *124*, 8825−8833.

(10) Vandemeulebroucke, A.; Versees, W.; De Vos, S.; Van Holsbeke, E.; Steyaert, J. *Biochemistry* **2003**, *42*, 12902−12908.

(11) Versees, W.; Steyaert, J. *Curr. Opin. Struct. Biol.* **2003**, *13*, 731−738.

(12) Birck, M. R.; Schramm, V. L. *J. Am. Chem. Soc.* **2004**, *126*, 2447−2453.

(13) (a) Lewandowicz, A.; Schramm, V. L. *Biochemistry* **2004**, *43*, 1458−1468. (b) Wielgus-Kutrowska, B.; Bzowska, A. *Biochim. Biophys. Acta* **2006**, *1764*, 887−902.

(14) Norman, R. A.; Barry, S. T.; Bate, M.; Breed, J.; Colls, J. G.; Ernill, R. J.; Luke, R. W. A.; Minshull, C. A.; McAlister, M. S. B.; McCall, E. J.; McMiken, H. H. J.; Paterson, D. S.; Timms, D.; Tucker, J. A.; Pauptit, R. A. *Structure* **2004**, *12*, 75−84.

(15) Hunt, C.; Gillani, N.; Farone, A.; Rezaei, M.; Kline, P. C. *Biochim. Biophys. Acta* **2005**, *1751*, 140−149.

(16) Loverix, S.; Versees, W.; Steyaert, J.; Geerlings, P. *Int. J. Quantum Chem.* **2005**, *106*, 565−570.

(17) Loverix, S.; Geerlings, P.; McNaughton, M.; Augustyns, K.; Vandemeulebroucke, A.; Steyaert, J.; Versees, W. *J. Biol. Chem.* **2005**, *280*, 14799−14802.

(18) Schramm, V. L. *Arch. Biochem. Biophys.* **2005**, *433*, 13−26.

(19) Bates, C.; Kendrick, Z.; McDonald, N.; Kline, P. C. *Phytochemistry* **2006**, *67*, 5−12.

(20) Kline, P. C.; Schramm, V. L. *Biochemistry* **1993**, *32*, 13212−13219.

(21) Mendieta, J.; Martin-Santamaria, S.; Priego, E.-M.; Balzarini, J.; Camarasa, M.-J.; Perez-Perez, M.-J.; Gago, F. *Biochemistry* **2004**, *43*, 405−414.

(22) Schyman, P.; Danielsson, J.; Pinak, M.; Laaksonen, A. *J. Phys. Chem. A* **2005**, *109*, 1713−1719.

(23) Deng, H.; Murkin, A. S.; Schramm, V. L. *J. Am. Chem. Soc.* **2006**, *128*, 7765−7771.

(24) (a) Horenstein, B. A.; Parkin, D. W.; Estupinan, B.; Schramm, V. L. *Biochemistry* **1991**, *30*, 10788−10795. (b) Parkin, D. W.; Mentch, F.; Banks, G. A.; Horenstein, B. A.; Schramm, V. L. *Biochemistry* **1991**, *30*, 4586−4594.

(25) Horenstein, B. A.; Schramm, V. L. *Biochemistry* **1993**, *32*, 7089−7097.

(26) (a) Versees, W.; Loverix, S.; Vandemeulebroucke, A.; Geerlings, P.; Steyaert, J. *J. Mol. Biol.* **2004**, *338*, 1−6. (b) Shivakumar, D. M.; Bruice, T. C. *Biochemistry* **2005**, *44*, 7805−7817.

(27) (a) Muzzolini, L.; Versees, W.; Tornaghi, P.; Van Holsbeke, E.; Steyaert, J.; Degano, M. *Biochemistry* **2006**, *45*, 773−782. (b) Versees, W.; Barlow, J.; Steyaert, J. *J. Mol. Biol.* **2006**, *359*, 331−346.

(28) Roday, S.; Amukele, T.; Evans, G. B.; Tyler, P. C.; Furneaux, R. H.; Schramm, V. L. *Biochemistry* **2004**, *43*, 4923−4933.

(29) (a) Mauro, D. J.; De Riel, J. K.; Tallarida, R. J.; Sirover, M. A. *Mol. Pharmacol.* **1993**, *43*, 854−857. (b) Hatahet, Z.; Kow, Y. W.; Purmal, A. A.; Cunningham, R. P.; Wallace, S. S. *J. Biol. Chem.* **1994**, *269*, 18814−18820. (c) Zastawny, T. H.; Doetsch, P. W.; Dizdaroglu, M. *FEBS Lett.* **1995**, *364*, 255−258. (d) Luo, N.; Mehler, E.; Osman, R. *Biochemistry* **1999**, *38*, 9209−9220. (e) Dinner, A. R.; Blackburn, G. M.; Karplus, M. *Nature* **2001**, *413*, 752−755. (f) Jiang, Y. L.; McDowell, L. M.; Poliks, B.; Studelska, D. R.; Cao, C.; Potter, G. S.; Schaefer, J.; Song, F.; Stivers, J. T. *Biochemistry* **2004**, *43*, 15429−15438.

(30) (a) Dodson, M. L.; Michaels, M. L.; Lloyd, R. S. *J. Biol. Chem.* **1994**, *269*, 32709−32712. (b) Savva, R.; McAuley-Hecht, K.; Brown, T.; Pearl, L. *Nature* **1995**, *373*, 487−493. (c) Kimura, E.; Kitamura, H.; Koike, T.; Shiro, M. *J. Am. Chem. Soc.* **1997**, *119*, 10909−10919. (d) McCullough, A. K.; Dodson, M. L.; Lloyd, R. S. *Annu. Rev. Biochem.* **1999**, *68*, 255−285. (e) Werner, R. M.; Jiang, Y. L.; Gordley, R. G.; Jagadeesh, G. J.; Ladner, J. E.; Xiao, G.; Tordova, M.; Gilliland, G. L.; Stivers, J. T. *Biochemistry* **2000**, *39*, 12585−12594. (f) Stivers, J. T.; Drohat, A. C. *Arch. Biochem. Biophys.* **2001**, *396*, 1−9. (g) Jiang, Y. L.; Drohat, A. C.; Ichikawa, Y.; Stivers, J. T. *J. Biol. Chem.* **2002**, *277*, 15385−15392. (h) Jiang, Y. L.; Ichikawa, Y.; Stivers, J. T. *Biochemistry* **2002**, *41*, 7116−7124.

(31) Parikh, S. S.; Walcher, G.; Jones, G. D.; Slupphaug, G.; Krokan, H. E.; Blackburn, G. M.; Tainer, J. A. *Proc. Natl. Acad. Sci. U.S.A.* **2000**, *97*, 5083−5088.

(32) Bianchet, M. A.; Seiple, L. A.; Jiang, Y. L.; Ichikawa, Y.; Amzel, L. M.; Stivers, J. T. *Biochemistry* **2003**, *42*, 12455−12460.

(33) (a) Porello, S. L.; Williams, S. D.; Kuhn, H.; Michaels, M. L.; David, S. S. *J. Am. Chem. Soc.* **1996**, *118*, 10684−10692. (b) Williams, S. D.; David, S. S. *Biochemistry* **2000**, *39*, 10098−10109. (c) Fromme, J. C.;

Banerjee, A.; Huang, S. J.; Verdine, G. L. *Nature* **2004**, *427*, 652−656. (d) Manuel, R. C.; Hitomi, K.; Arvai, A. S.; House, P. G.; Kurtz, A. J.; Dodson, M. L.; McCullough, A. K.; Tainer, J. A.; Lloyd, R. S. *J. Biol. Chem.* **2004**, *279*, 46930−46939.

(34) (a) Fromme, J. C.; Bruner, S. D.; Yang, W.; Karplus, M.; Verdine, G. L. *Nat. Struct. Biol.* **2003**, *10*, 204−211. (b) Norman, D. P. G.; Chung, S. J.; Verdine, G. L. *Biochemistry* **2003**, *42*, 1564−1572. (c) Lingaraju, G. M.; Sartori, A. A.; Kostrewa, D.; Prota, A. E.; Jiricny, J.; Winkler, F. K. *Structure* **2005**, *13*, 87−98.

(35) Osakabe, T.; Fujii, Y.; Hata, M.; Tsuda, M.; Neya, S.; Hoshino, T. *Chem−Bio Inf. J.* **2004**, *4*, 73−92.

(36) Rabow, L. E.; Kow, Y. W. *Biochemistry* **1997**, *36*, 5084−5096.

(37) (a) Fromme, J. C.; Verdine, G. L. *J. Biol. Chem.* **2003**, *278*, 51543−51548. (b) Zharkov, D. O.; Shoham, G.; Grollman, A. P. *DNA Repair* **2003**, *2*, 839−862. (c) Coste, F.; Ober, M.; Carell, T.; Boiteux, S.; Zelwer, C.; Castaing, B. *J. Biol. Chem.* **2004**, *279*, 44074−44083. (d) Fromme, J. C.; Banerjee, A.; Verdine, G. L. *Curr. Opin. Struct. Biol.* **2004**, *14*, 43−49. (e) Zaika, E. I.; Perlow, R. A.; Matz, E.; Broyde, S.; Gilboa, R.; Grollman, A. P.; Zharkov, D. O. *J. Biol. Chem.* **2004**, *279*, 4849−4861.

(38) (a) Schramm, V. L. *Biochim. Biophys. Acta* **2002**, *1587*, 107−117. (b) Deng, H.; Lewandowicz, A.; Schramm, V. L.; Callender, R. *J. Am. Chem. Soc.* **2004**, *126*, 9516−9517. (c) Nunez, S.; Antoniou, D.; Schramm, V. L.; Schwartz, S. D. *J. Am. Chem. Soc.* **2004**, *126*, 15720−15729. (d) Gao, X.-F.; Huang, X.-R.; Sun, C.-C. *J. Struct. Biol.* **2006**, *154*, 20−26.

(39) Canduri, F.; dos Santos, D. M.; Silva, R. G.; Mendes, M. A.; Basso, L. A.; Palma, M. S.; de Azevedo, W. F.; Santos, D. S. *Biochem. Biophys. Res. Commun.* **2004**, *313*, 907−914.

(40) Canduri, F.; Fadel, V.; Basso, L. A.; Palma, M. S.; Santos, D. S.; de Azevedo, W. F. *Biochem. Biophys. Res. Commun.* **2005**, *327*, 646−649.

(41) (a) Bruner, S. D.; Norman, D. P. G.; Verdine, G. L. *Nature* **2000**, *403*, 859−866. (b) Norman, D. P. G.; Bruner, S. D.; Verdine, G. L. *J. Am. Chem. Soc.* **2001**, *123*, 359−360. (c) Norman, D. P. G.; Chung, S. J.; Verdine, G. L. *Biochemistry* **2003**, *42*, 1564−1572. (d) Lingaraju, G. M.; Sartori, A. A.; Kostrewa, D.; Prota, A. E.; Jiricny, J.; Winkler, F. K. *Structure* **2005**, *13*, 87−98. (e) Kuznetsov, N. A.; Koval, V. V.; Zharkov, D. O.; Nevinsky, G. A.; Douglas, K. T.; Fedorova, O. S. *Nucleic Acids Res.* **2005**, *33*, 3919−3931.

(42) Di Laudo, M.; Whittleton, S. R.; Wetmore, S. D. *J. Phys. Chem. A* **2003**, *107*, 10406−10413.

(43) (a) Whittleton, S. R.; Hunter, K. C.; Wetmore, S. D. *J. Phys. Chem. A* **2004**, *108*, 7709−7718. (b) McConnell, T. L.; Wheaton, C. A.; Hunter, K. C.; Wetmore, S. D. *J. Phys. Chem. A* **2005**, *109*, 6351−6362. (c) Hunter, K. C.; Rutledge, L. R.; Wetmore, S. D. *J. Phys. Chem. A* **2005**, *109*, 9554−9562.

(44) (a) Becke, A. D. *J. Chem. Phys.* **1993**, *98*, 5648−5652. (b) Becke, A. D. *Phys. Rev. A* **1988**, *38*, 3098−3100. (c) Lee, C. T.; Yang, W. T.; Parr, R. G. *Phys. Rev. B* **1988**, *37*, 785−789.

(45) The H4′−C4′−C5′−O5′ dihedral angle is approximately equal to 180° in DNA, and therefore the hydroxyl and methoxyl groups were added in the same orientation in our models. However, we note that many enzymes catalyze a base flipping step prior to glycosidic bond cleavage, which changes the alignment of the phosphodiester backbone.

(46) Boys, S. F.; Bernardi, F. *Mol. Phys.* **1970**, *19*, 553.

(47) Frisch, M. J.; Trucks, G. W.; Schlegel, H. B.; Scuseria, G. E.; Robb, M. A.; Cheeseman, J. R.; Montgomery, J. A., Jr.; Vreven, T.; Kudin, K. N.; Burant, J. C.; Millam, J. M.; Iyengar, S. S.; Tomasi, J.; Barone, V.; Mennucci, B.; Cossi, M.; Scalmani, G.; Rega, N.; Petersson, G. A.; Nakatsuji, H.; Hada, M.; Ehara, M.; Toyota, K.; Fukuda, R.; Hasegawa, J.; Ishida, M.; Nakajima, T.; Honda, Y.; Kitao, O.; Nakai, H.; Klene, M.; Li, X.; Knox, J. E.; Hratchian, H. P.; Cross, J. B.; Bakken, V.; Adamo, C.; Jaramillo, J.; Gomperts, R.; Stratmann, R. E.; Yazyev, O.; Austin, A. J.; Cammi, R.; Pomelli, C.; Ochterski, J. W.; Ayala, P. Y.; Morokuma, K.; Voth, G. A.; Salvador, P.; Dannenberg, J. J.; Zakrzewski, V. G.; Dapprich, S.; Daniels, A. D.; Strain, M. C.; Farkas, O.; Malick, D. K.; Rabuck, A. D.; Raghavachari, K.; Foresman, J. B.; Ortiz, J. V.; Cui, Q.; Baboul, A. G.; Clifford, S.; Cioslowski, J.; Stefanov, B. B.; Liu, G.; Liashenko, A.; Piskorz, P.; Komaromi, I.; Martin, R. L.; Fox, D. J.; Keith, T.; Al-Laham, M. A.; Peng, C. Y.; Nanayakkara, A.; Challacombe, M.; Gill, P. M. W.; Johnson, B.; Chen, W.; Wong, M. W.; Gonzalez, C.; Pople, J. A. *Gaussian 03*, revision C.02 and D.01; Gaussian, Inc.: Wallingford, CT, 2004.

(48) It has been determined experimentally that the sugar puckering for RNA and A-DNA is C3′-endo, while it is C2′-endo in B-DNA.

(49) We note that the IRCs typically lead to reactant complexes with C3′-endo sugar puckering and the energy difference between the C3′-endo and the C2′-endo conformations is small, where model **1** predicts the C3′-endo conformation to be 5 kJ mol^{-1} more stable and model **4-CH$_3$** predicts C2′-endo to be 1 kJ mol^{-1} more stable. Since conversion between different sugar conformations is expected to be a low-energy process, we utilized reactant complexes with C3′-endo puckering in all pathways for consistency.

(50) Gelbin, A.; Schneider, B.; Clowney, L.; Hsieh, S. H.; Olson, W. K.; Berman, H. M. *J. Am. Chem. Soc.* **1996**, *118*, 519−529.

(51) Smar, M.; Short, S. A.; Wolfenden, R. *Biochemistry* **1991**, *30*, 7908−7912.

(52) Although IRCs for the first and second steps should ideally lead to the same intermediate complex, two structures with slightly different water orientations were obtained for model **4-CH$_3$**, which differ by only 1.4 kJ mol^{-1}. Since we expect a low barrier for water migration, we report only the relative energy for the intermediate obtained by following the IRC from the first step.

(53) (a) Bruner, M.; Horenstein, B. A. *Biochemistry* **2000**, *39*, 2261−2268. (b) Lee, J. K.; Bain, A. D.; Berti, P. J. *J. Am. Chem. Soc.* **2004**, *126*, 3769−3776.

(54) (a) Parkin, D. W.; Schramm, V. L. *Biochemistry* **1987**, *26*, 913−920. (b) Huang, X.; Tanaka, K. S. E.; Bennet, A. J. *J. Am. Chem. Soc.* **1997**, *119*, 11147−11154. (c) Scheuring, J.; Schramm, V. L. *Biochemistry* **1997**, *36*, 8215−8223. (d) Scheuring, J.; Schramm, V. L. *Biochemistry* **1997**, *36*, 4526−4534. (e) Rising, K. A.; Schramm, V. L. *J. Am. Chem. Soc.* **1997**, *119*, 27−37. (f) Yang, J.; Schenkman, S.; Horenstein, B. A. *Biochemistry* **2000**, *39*, 5902−5910. (g) Parikh, S. L.; Schramm, V. L. *Biochemistry* **2004**, *43*, 1204−1212.

(55) Zhao, Y.; Pu, J. Z.; Lynch, B. J.; Truhlar, D. G. *Phys. Chem. Chem. Phys.* **2004**, *6*, 673−676.

(56) Durant, J. L. *Chem. Phys. Lett.* **1996**, *256*, 595−602.

(57) Lynch, B. J.; Fast, P. L.; Harris, M.; Truhlar, D. G. *J. Phys. Chem. A* **2000**, *104*, 4811−4815.

(58) Truong, T. N.; Duncan, W. *J. Chem. Phys.* **1994**, *101*, 7408−7414.

(59) Becke, A. D. *J. Chem. Phys.* **1993**, *98*, 1372−1377.

(60) Zhao, Y.; Truhlar, D. G. *J. Phys. Chem. A* **2004**, *108*, 6908−6918.

(61) Zhao, Y.; Gonzalez-Garcia, N.; Truhlar, D. G. *J. Phys. Chem. A* **2005**, *109*, 2012−2018.

(62) Zhao, Y.; Truhlar, D. G. *J. Phys. Chem. A* **2005**, *109*, 5656−5667.

(63) Zhang, R. B.; Somers, K. R. F.; Kryachko, E. S.; Nguyen, M. T.; Zeeger-Huyskens, T. S.; Ceulemans, A. *J. Phys. Chem. A* **2005**, *109*, 8028−8034.

(64) The 6-311+G(2df,2p) basis set was used in conjunction with MPWB1K, MPW1B95, and PWB6K hybrid density functional methods as implemented in Truhlar's benchmarking studies (see refs 60−62).